

# Missing iris effect as a possible cause of muted hydrological change and high climate sensitivity in models

Thorsten Mauritsen\* and Bjorn Stevens

**Equilibrium climate sensitivity to a doubling of CO<sub>2</sub> falls between 2.0 and 4.6 K in current climate models, and they suggest a weak increase in global mean precipitation. Inferences from the observational record, however, place climate sensitivity near the lower end of this range and indicate that models underestimate some of the changes in the hydrological cycle. These discrepancies raise the possibility that important feedbacks are missing from the models. A controversial hypothesis suggests that the dry and clear regions of the tropical atmosphere expand in a warming climate and thereby allow more infrared radiation to escape to space. This so-called iris effect could constitute a negative feedback that is not included in climate models. We find that inclusion of such an effect in a climate model moves the simulated responses of both temperature and the hydrological cycle to rising atmospheric greenhouse gas concentrations closer to observations. Alternative suggestions for shortcomings of models — such as aerosol cooling, volcanic eruptions or insufficient ocean heat uptake — may explain a slow observed transient warming relative to models, but not the observed enhancement of the hydrological cycle. We propose that, if precipitating convective clouds are more likely to cluster into larger clouds as temperatures rise, this process could constitute a plausible physical mechanism for an iris effect.**

In the tropics, radiative cooling predominantly occurs in dry and clear subsiding parts of the atmosphere. The radiative cooling is balanced mainly by latent heat released in precipitating deep convective clouds (Fig. 1). Processes that may change the balance in favour of dry and clear regions in warmer climates have been proposed to constitute a possible negative feedback not represented by climate models<sup>1</sup>. This potential feedback has been termed the iris effect, in analogy to the enlargement of the eye's iris as its pupil contracts under the influence of more light (Box 1). It is unclear, however, whether an iris effect can be directly detected in observed variations of tropical cloud<sup>1,2</sup>, precipitation<sup>3–5</sup> or radiation fields<sup>6–8</sup> that co-vary with sea surface temperature. We approach the question differently, and instead investigate whether the presence of an iris effect would lead to other physical changes that might be more readily observed. We suggest that candidate changes are a possibility of a low-end climate sensitivity despite positive shortwave cloud feedback, and enhanced precipitation increases with warming to balance atmospheric cooling associated with an iris effect.

## Past debate on the iris effect

Observations of natural variations of upper-level cloud cover with underlying sea surface temperatures over the warm-pool region in the western Pacific led to the conceptual idea of an iris effect. Cloud cover was found to be reduced by about 22% per degree warming<sup>1</sup>. Although the magnitude of the reduction is somewhat dependent on methodology, the sign is robust<sup>9,10</sup>. A reduced upper-level cloud cover with warmer surface temperatures could constitute a negative feedback on climate change, because thin and cold high-level ice clouds have a net warming effect (Box 1).

Taking a high-cloud reducing effect of a warming sea surface into account has led to an estimate of the equilibrium climate sensitivity (ECS) — the expected long-term surface warming associated with a doubling of atmospheric CO<sub>2</sub> — of only about 1 K (ref. 1). This is

well below that of any climate model and also below the 1.5 K that is generally thought to be the lowest possible ECS based on various lines of evidence<sup>11</sup>. But this low ECS-estimate is conditional not only on the rate of reduction of high-level clouds, but also on cloud optical properties (Box 1). The cooling implied by the iris effect is strongest if the thinnest clouds diminish. If it is instead primarily the thicker anvils that are reduced in a warmer climate, the negative feedback of the iris effect is weaker<sup>12,13</sup>.

Detection of an iris effect in observations is not straightforward. Convection preferentially occurs over the warmest surface temperatures, which makes it challenging to interpret natural variations. If an analysis focuses on small regions, it may appear as if upper-level cloud cover increases with temperature, despite an average decrease at a larger scale. The observed cloud reductions that accompanied an increase in the surface temperature within convecting regions<sup>1</sup> occurred thousands of kilometres away from the location where the actual convection occurred<sup>2</sup>, which raised questions about the causal relationship between these changes. But depending on the scale at which tropical convection organizes, this clearing in the surroundings can be interpreted as an expansion of the associated dry and clear regions.

Patterns of local warming can be associated with circulation changes that one would not expect in a warming climate, and unravelling whether changes in cloudiness are the cause or the consequence of the circulation changes is not straightforward<sup>14</sup>.

## Monthly variations of the tropical energy budget

Alternatively, fluctuations in the top-of-atmosphere radiation balance that accompany surface temperature fluctuations can be studied directly, and constitute a potential feedback<sup>14,15</sup>. An updated analysis is focused on the tropics (Fig. 2) because this region is central to the debate over the iris effect<sup>6–8</sup>. When temperatures are anomalously warm, the surface emits more longwave radiation to

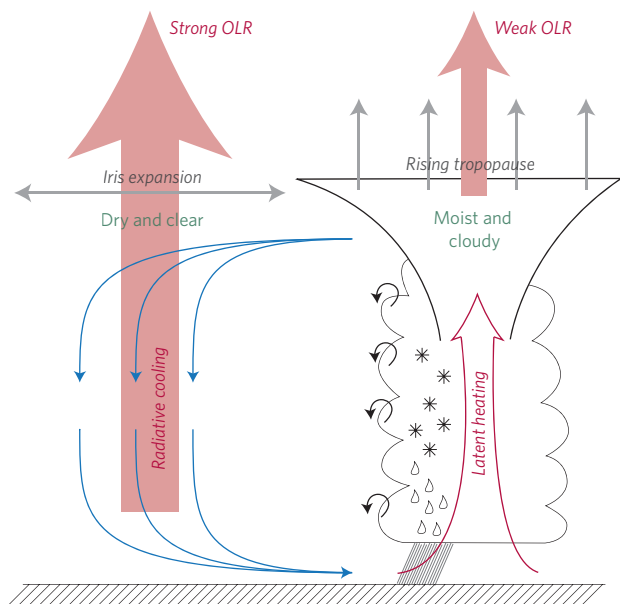


**Figure 1** | Illustration of the tropical atmospheric circulation.

cool off. But the strength of the net temperature restoration depends on atmospheric feedback mechanisms. In the case of open domains such as the one analysed here, lateral fluxes of energy out of the domain can change.

Satellite data from the Clouds and the Earth's Radiant Energy System (CERES) instruments show a strong negative longwave regression close to the Planck feedback in the tropics<sup>16</sup>, and a weak positive shortwave regression to yield a net regression of  $-3.2 \pm 1.0 \text{ W m}^{-2} \text{ K}^{-1}$  (Fig. 2, Supplementary Table 2). The ensemble mean of the climate models of the fifth phase of the Coupled Model Intercomparison Project (CMIP5) matches the observed relationship between temperature and net shortwave radiation, albeit with considerable scatter, but systematically exhibits a longwave regression that is too weak (Fig. 2b, Supplementary Table 3). Analysis of irradiances measured in cloud-free regions reveals that the discrepancy in the longwave radiation is due to both water vapour and clouds, with the latter dominating. The regression coefficients are sensitive to methodological details, for instance the treatment of volcanoes<sup>7,15</sup>, or the lag (or no lag) in the radiative response relative to temperature changes<sup>8</sup>, but the discrepancy between the observations on the one hand and the models on the other is robust.

The relationship between the slope of the regression of net radiation against temperature and ECS is not strong. Reference 8 provides estimates of ECS from a set of 11 previous-generation CMIP3 models, as well as the actual ECS based on  $\text{CO}_2$ -doubling experiments. Omitting one model with infinite estimated ECS, a dissatisfying correlation between estimated and actual ECS of  $-0.11$  is found, making it difficult to argue that a more negative regression coefficient between monthly anomalies of net radiation and temperature per se implies a smaller ECS. In the analysis of the CMIP5 ensemble presented here, we obtain stronger correlations of  $+0.42$  and  $+0.15$  between net regression and the inverse ECS for the Atmospheric Model Intercomparison Project (AMIP) and historical experiments, respectively (Supplementary Table 3). Of the nine models that match CERES net regression in either experiment, three have ECS above 3 K and six below. Only the two versions of the Beijing Climate Center (BCC) model match observations in the slope of the regression between net, longwave and shortwave radiation with temperature, and only if run with a prescribed evolution of sea surface temperatures (AMIP). If run in coupled mode (historical) the model is far from matching CERES data.

Thus, whereas the discrepancy between the model ensemble and observations is suggestive of missing processes, the analysis of monthly variability in the tropical radiation budget poses at best weak constraints on global ECS.

### Convective aggregation as a possible mechanism

One objection to the idea of an iris effect is that it is not clear what the physical mechanism might be. An iris effect could result if the efficiency of precipitation within deep convective cloud towers increased with warming, leading to less detrainment into their anvils<sup>5,17</sup>. This could occur if aggregation of convective clouds into large clusters is temperature-dependent. Aggregation is due to an instability of radiative-convective equilibrium, whereby relatively dry regions cool radiatively, resulting in local subsidence and further suppression of convection, ultimately leading to an aggregated state with localized convective clusters<sup>18</sup>. The cooling of the dry and clear regions is expected to increase with warmer temperatures and hence promote aggregation<sup>19</sup>. In addition, in a warmer climate convective clouds may further be invigorated by enhanced latent heat release<sup>20</sup>.

As larger convective clouds dilute less by lateral mixing they precipitate more of their water during ascent, and fewer large clusters can provide the necessary latent heating to sustain atmospheric radiative cooling (Fig. 1). Both cloud-resolving simulations<sup>21</sup> and observations<sup>22</sup> confirm that outgoing longwave radiation does increase as a consequence of a drying environment in more aggregated states. Shortwave absorption also increases, which tends to cancel some of the effect. All in all, however, we conclude that it is plausible that convective aggregation constitutes a negative longwave feedback on climate change — and to our understanding, the underlying processes are not explicitly represented in climate models.

In principle, the problem of convective aggregation lends itself to fine-scale simulations that explicitly resolve the dynamics of individual convective clouds. In small-domain simulations, however, whether or not convection will aggregate depends critically on resolution, domain-size and initial conditions<sup>23</sup>. This complicates the interpretation of possible temperature dependencies. Pioneering work to simulate convective clouds at the global scale has suggested a somewhat puzzling combined upper-level reduction in cloud ice with an increase in cloud cover in response to warming<sup>24</sup>. But the model's feedback is highly sensitive to the representation of physical processes that remain unresolved. Cloud microphysics, in particular, represents a challenge to the application of fine-scale simulations<sup>25</sup>.

### Climate model test with a simple parameterization

Convective processes that could give rise to an iris effect are crudely represented in most global climate models. Despite some progress in understanding how convective aggregation could be enhanced at warmer temperatures, knowledge of how to incorporate such processes remains primitive. For this reason, we simply scale the conversion rate from cloud water to rain ( $C_p$ ) in convective clouds in the ECHAM6 atmosphere general circulation model (Supplementary Methods) with local surface temperature, similar to a previous approach<sup>17</sup>:

$$C_p(T_s) = C_0 (1 + I_c)^{T_s - T_0} \quad (1)$$

where  $C_0 = 2 \times 10^{-4} \text{ s}^{-1}$  is the default conversion rate in ECHAM6,  $T_s$  is surface temperature, and  $T_0$  is a reference temperature set to  $25 \text{ }^\circ\text{C}$  — a value typically found in the tropics. The parameter  $I_c$  is included to control the strength of the iris effect, and is here set to 0.2, 0.5 and 1.0, corresponding in the most extreme case to a doubling of the conversion rate per degree warming. Because the rate at which cloud water is converted to precipitation in convective clouds is not a directly observable quantity, but is important for the behaviour of the parameterization, it is frequently used as a tuning

**Box 1 | The tropical circulation and the iris effect.**

The tropical atmosphere consists of moist and cloudy regions associated with large-scale rising motion, convective storms and pronounced precipitation on the one hand, and dry and clear regions with subsiding motion on the other hand (Fig. 1). The atmospheric circulation maintains an approximate balance between radiative cooling, which occurs preferentially in the dry and clear regions, and latent heating from the condensation of water vapour in precipitating clouds. As a conceptual starting point, convection occurs in a narrow intertropical convergence zone (ITCZ) near the Equator and subsidence is predominant in the subtropics, although the reality is, of course, more complicated.

Shifts in the tropical circulation in a warming climate can act either to amplify or to dampen the temperature change through feedback mechanisms. Positive and well-understood feedbacks arise; for example, specific humidity increases in a warmer climate, and the altitude of convective cloud tops rises. Both these feedbacks act to reduce the outgoing longwave radiation (OLR), and thereby amplify surface warming.

The controversial ‘iris hypothesis’ proposes that the fraction of the dry and clear regions could increase with warming<sup>1</sup> and exert a negative feedback: a larger extent of the dry and clear regions would lead to a less cloudy upper troposphere and hence an increase in OLR. Such an effect could mitigate against climate

change. But a drier upper troposphere would also allow more solar radiation to be absorbed by the Earth and atmosphere, rather than reflected back to space by the clouds, so that the net effect of reducing high clouds is not obvious<sup>12,13</sup>. On balance, the effect is thought to be negative.

Evidence for an iris effect is found in observations of tropical variability of upper-level cloud cover, precipitation and the radiation balance co-varying with natural variations of the surface temperature. These findings have led to estimates<sup>1,8</sup> of the sensitivity of surface temperature to a doubling of atmospheric CO<sub>2</sub> concentrations of only about 1 K, much lower than the broadly accepted range of 1.5–4.5 K (ref. 11). The estimate of ECS with an iris effect, however, depends not only on the rate of reduction of high-level clouds, but also on the cloud optical properties of the most sensitive clouds. If the thinnest clouds are preferentially removed, the effect on outgoing longwave radiation is stronger than that on reflectivity, and the iris effect is stronger. On the other hand, if the reduction in cloud cover affects thicker clouds more strongly, the loss in reflectivity plays a more important role, and the iris effect is less pronounced.

Notwithstanding its exact strength, the evidence for an iris effect has been contested, and the lack of a clear physical mechanism has caused widespread scepticism.

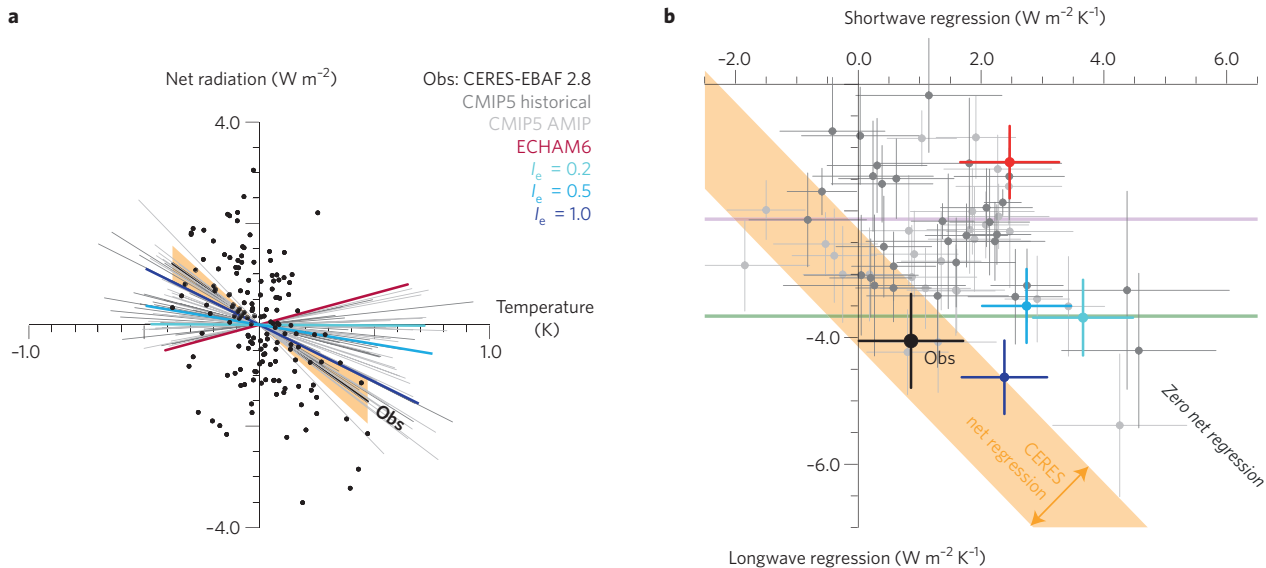


**Figure 2 | Regression lines calculated from anomalies of top of atmosphere radiation versus surface temperature in the tropics (20°S to 20°N).**

**a**, De-trended monthly mean de-seasonalized anomalies (shown as black dots) of observed net radiation (CERES-EBAF 2.8) against surface temperature (HadCRUT4) for the full years 2001–2013. The black line shows a linear regression on the data, and orange is the 5–95% confidence interval obtained from a two-sided *t*-test. Regressions from models are shown as grey and coloured lines according to the legend and are performed for the period 1995–2005 to avoid the influence of the Pinatubo eruption. **b**, The relation between the shortwave and longwave contributions to net regression. Error bars indicate 5–95% confidence intervals on the regression coefficients. In the *t*-test we account for temporal autocorrelation in the surface temperature record of about 10 months. Longwave Planck feedback (green) of  $-3.94 \text{ W m}^{-2} \text{ K}^{-1}$  and Planck feedback plus water vapour feedback evaluated at constant relative humidity (pink) of  $-2.12 \text{ W m}^{-2} \text{ K}^{-1}$  for the tropical region, 20°N to 20°S, are obtained from ref. 16.

parameter, and as such has been varied by almost two orders of magnitude<sup>26</sup>. By comparison, the changes introduced through our simple parameterization, equation (1), are small. With these settings, in particular the choice of  $T_o$ , the present-day mean climate of ECHAM6-Iris is not appreciably different from that of the original model (Supplementary Figs 1–5 and Supplementary Table 1). Moreover, because precipitation outside the tropics is foremost carried by the large-scale cloud scheme, mid-latitude storms and

circulation are not directly affected much by the modification. The approach is clearly simplistic, but allows an exploration of the implications of an iris effect in a simple and controllable way. Indeed, we find that whereas ECHAM6 was among the largest outliers in its representation of month-to-month tropical co-variability in radiation and surface temperature (Fig. 2), all three settings of  $I_e$  yield longwave regression coefficients in statistical agreement with the data.

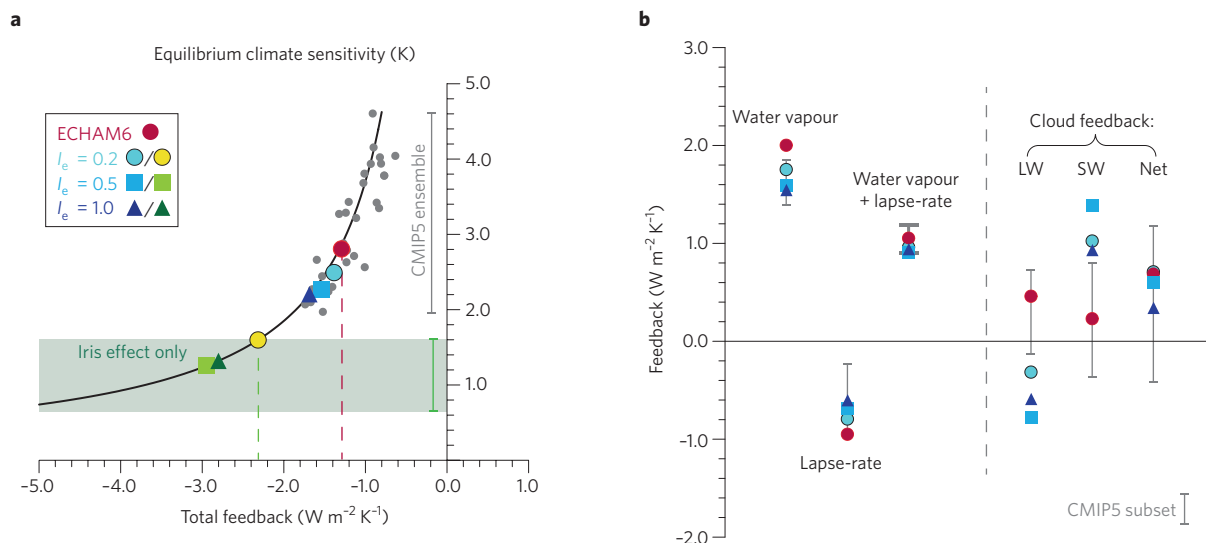


**Figure 3 | Decomposition of feedback into individual mechanisms that control variations in model equilibrium climate sensitivity.** **a**, ECS is inversely proportional to the total feedback, as indicated by the solid black line, whereby the forcing is assumed to be  $3.7 \text{ W m}^{-2}$  for a doubling of  $\text{CO}_2$ . The grey filled circles are values for the individual CMIP5 climate models estimated by linear extrapolation to equilibrium in the idealized experiment with abruptly quadrupled  $\text{CO}_2$ . The CMIP5 results are divided by two to be comparable to a doubling of  $\text{CO}_2$  as applied here. The pale green range is that suggested by ref. 1. Green and yellow symbols are diagnosed estimates of climate sensitivity given only the change in water vapour feedback and longwave cloud feedback for each value of  $I_e$ . **b**, Decomposition by partial radiative perturbations of the total feedback into components that are due to change in water vapour, lapse-rate, surface albedo and clouds (see Supplementary Methods). Cloud feedback is further split into longwave (LW) and shortwave (SW) components. Planck and surface albedo feedback (not shown) do not vary substantially with  $I_e$ . Ranges of feedbacks are from a subset of 11 CMIP5 models estimated by the radiative kernel method<sup>28</sup>; systematic differences may be due to different methodologies.

### Climate sensitivity

Equilibrium climate sensitivity is inversely proportional to total feedback, which in turn can be split into individual additive feedback mechanisms (Fig. 3). Robust and well-understood positive feedback mechanisms — such as the increase in absolute humidity that accompanies a rise in temperature at fixed relative humidity; lowered surface solar reflection due to a reduction in surface snow and ice; and a positive feedback associated with rising convective anvil clouds in a warming climate — together yield a null-hypothesis ECS around 2.7 K (ref. 27). This estimate neglects uncertain shortwave cloud feedbacks<sup>28</sup>, and a possible iris effect. If cloud shortwave feedbacks are positive<sup>29–33</sup>, ECS would be larger and fall in the range of 3 to 5 K. If one further assumes that a lower ECS is associated with a better match between model output and the observed record<sup>34–36</sup>, then an additional unrepresented negative feedback, such as an iris effect, is required.

The standard version of ECHAM6 has an ECS of 2.8 K to a doubling of  $\text{CO}_2$  (Fig. 3a), consistent with the null-hypothesis<sup>27</sup> plus a small positive shortwave cloud feedback (Fig. 3b). To achieve a climate sensitivity in line with the estimated range suggested for an active iris effect<sup>1</sup> would require to change the total feedback of ECHAM6 by more than  $-1.0 \text{ W m}^{-2} \text{ K}^{-1}$  (Fig. 3a, dashed lines). ECHAM6-Iris exhibits a reduction of the water vapour and cloud longwave feedbacks of together  $-1.0$  to  $-1.8 \text{ W m}^{-2} \text{ K}^{-1}$  depending on  $I_e$ , which alone is sufficient to produce an ECS between 1.2 and 1.6 K (Fig. 3, green symbols). Thus, ECHAM6-Iris exhibits a strong iris effect, as designed, with a negative longwave cloud feedback clearly outside the range of present modelling.

The reduction in the positive water vapour feedback is largely compensated, however, by a weakening of the negative lapse-rate feedback associated with a less amplified warming of the upper troposphere; this type of compensation arises also in other models. Only considering lapse-rate compensation would yield a somewhat higher ECS of 1.4–1.7 K. A weakening of the lapse rate feedback (Supplementary Figs 7 and 8), although small, is in line with observations of tropical tropospheric temperature trends suggesting

weaker warming aloft than commonly found in models<sup>37,38</sup>. In addition to a weaker lapse-rate feedback, ECHAM6-Iris exhibits an enhanced positive shortwave cloud feedback such that the net cloud feedback is only slightly reduced in the global mean (Fig. 3b, Supplementary Figs 3–5). Together, these mechanisms compensate the strong negative feedbacks associated with longwave cloud radiative effects, so that the resulting reduction of ECS (from 2.8 K to 2.2–2.5 K) is relatively modest (Fig. 3a, Supplementary Fig. 6).

Cloud shortwave feedback compensation is the most important countervailing factor responsible for the moderation of ECS when including an iris effect. Some shortwave compensation was originally assumed from the anvil cloud reduction<sup>1</sup>, but seems to have been underestimated<sup>12,13</sup>. We find a reduction of cloud fraction and cloud condensate not only in regions of deep convection but virtually everywhere, associated with a general drying of the atmosphere (Supplementary Figs 12–15), such that shortwave compensation dominates in the sub- and extratropics (Supplementary Figs 9–11).

Even though deep convection occurs predominantly in the tropics, the enhanced conversion is evident globally. And although the strength of the shortwave cloud compensation could differ from what is produced by ECHAM6, some compensation seems inevitable. It is hard to imagine an atmosphere with an iris effect that does not dry in terms of relative humidity. In fact, over-compensation by shortwave cloud feedback was found when including Equation (1) in the NCAR climate model: the result was a rise in ECS (A. Gettelman, personal communication). Together, our findings of a robust lapse-rate compensation and the likelihood of a positive shortwave cloud feedback suggest that the current consensus lower bound of 1.5 K for the ECS<sup>11</sup> may be a conservative choice.

### Hydrological sensitivity

Changes to the global mean hydrological cycle are tied to the atmospheric energy budget<sup>39,40</sup>, whereby increased radiative cooling of the atmosphere under global warming is predominantly balanced by latent heating through precipitation (Fig. 1). An iris effect is predicted to increase hydrological sensitivity, because the longwave radiative

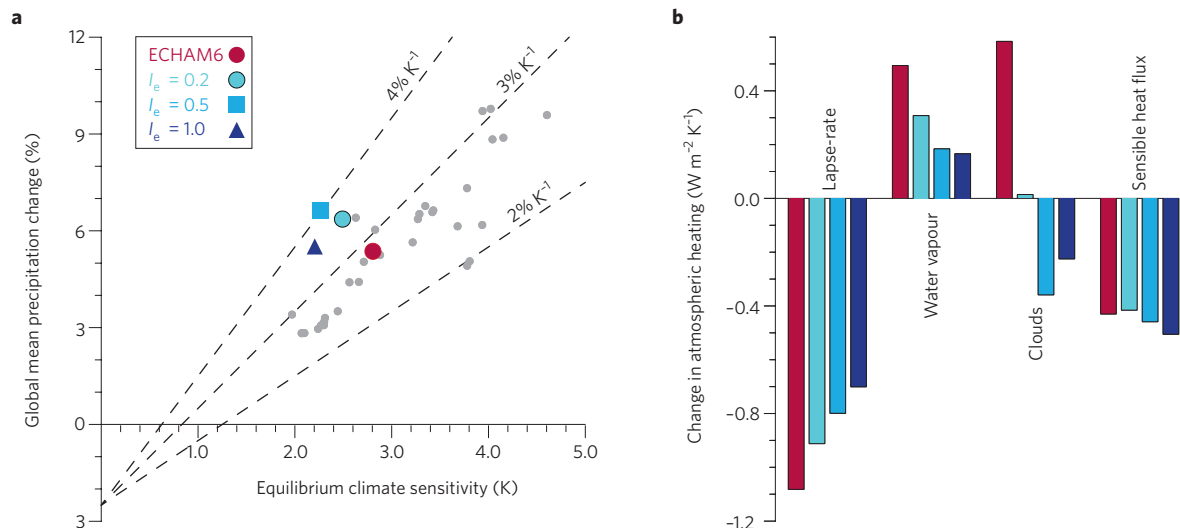


**Figure 4 | Analysis of hydrological sensitivity and a separation into the contributions from individual mechanisms.** **a**, Global mean precipitation change for 32 coupled CMIP5 models in experiments with abruptly quadrupled  $\text{CO}_2$  are compared with the mixed-layer ocean simulations performed in this study by the use of linear extrapolation to equilibrium. Hydrological sensitivity is indicated by the dashed lines, although the initial suppression due to  $\text{CO}_2$  heating of the atmosphere is slightly model-dependent. The CMIP5 results are divided by two to be comparable to a doubling of  $\text{CO}_2$  as applied here. **b**, Decomposition of the change in the atmospheric energy heating per degree warming after reaching equilibrium with a doubling of  $\text{CO}_2$  (Supplementary Methods). For reference, a 1% increase in precipitation corresponds to about  $0.8\text{--}0.85 \text{ W m}^{-2}$  atmospheric heating. The effects of  $\text{CO}_2$ , Planck and surface albedo change are not substantially different among the models.

cooling of the atmosphere associated with reduced upper-level cloudiness must be balanced by enhanced latent heating by precipitation.

CMIP5 models exhibit a relatively narrow range in the rise of global mean precipitation of  $2.0\text{--}3.3\% \text{ K}^{-1}$  (Fig. 4); ECHAM6 has a mid-range hydrological sensitivity of  $2.9\% \text{ K}^{-1}$ . When including an iris effect, however, hydrological sensitivity is enhanced beyond the CMIP5 ensemble to around  $3.5\text{--}4\% \text{ K}^{-1}$  (Fig. 4a). The increase in the hydrological sensitivity is due mainly to clouds shifting from warming the atmosphere in ECHAM6 to cooling with an iris effect (Fig. 4b). Also, water vapour heats the atmosphere less in the drier atmosphere that accompanies an iris effect, and a slight reduction in surface sensible heat flux contributes to enhanced precipitation, too. On the other hand, the increase in hydrological sensitivity is dampened by a weakening lapse-rate feedback that leads to less radiative cooling of the atmosphere. Thus an iris effect could help to reconcile studies based on station data<sup>41</sup>, satellite observations<sup>42</sup>, ocean surface salinity change<sup>43</sup> and reconstructions<sup>44</sup> which, notwithstanding the large uncertainty in the measurements, have raised the question as to whether models collectively underestimate the rate at which precipitation increases globally with warming.

In a warming climate, wet regions in the deep tropics and in mid- and high latitudes are expected to get wetter whereas the dry subtropical regions get drier<sup>40</sup>. This tendency is also found in ECHAM6 and ECHAM6-Iris (Supplementary Figs 16 and 17). But whereas ECHAM6 sharpens the intertropical convergence zone (ITCZ), ECHAM6-Iris splits the ITCZ by drying near the Equator in the Pacific and wetting off the Equator. Likewise, the subtropical dry-zones move further poleward (Supplementary Fig. 18). This could help to reconcile models with observations of greater Hadley cell widening during recent warming<sup>45</sup>. Further, if convective aggregation is enhanced in warmer climates, one might speculate that extreme precipitation events could increase faster than the increase in available atmospheric water vapour of about  $7\% \text{ K}^{-1}$  (ref. 20), as larger storms can converge more water from the surrounding regions.

### Challenging alternatives

In the past, the slow observed warming consistent with lower-end ECS estimates has been explained by greater than anticipated aerosol

cooling<sup>46</sup>, a failure to incorporate forcing from recent volcanic eruptions<sup>47</sup>, or unobserved heat uptake by the deep ocean<sup>48</sup>. If anthropogenic or volcanic aerosols temporarily cool the Earth more, or heat flows faster into the deep oceans than expected, then the temperature response to rising  $\text{CO}_2$  is merely delayed with little impact on ECS itself. Such effects are consistent with a weaker rate of transient warming. None of them, however, can explain the higher observed hydrological sensitivity, because both  $\text{CO}_2$  and aerosol forcing heat the atmosphere by absorbing radiation<sup>49</sup>, acting to reduce global mean precipitation in the absence of significant surface warming. Furthermore, inferences about deep ocean heat uptake in the past decade are not able to detect a significant contribution from the ocean below the current observing system<sup>50</sup>.

In contrast, the iris hypothesis predicts a coherent pattern of the climate response to increasing atmospheric greenhouse gas concentrations, which helps to reconcile climate model simulations with observations in a number of respects. Our simulations with a simple parameterization of an effect akin to the iris effect combine realistic month-to-month variability of longwave fluxes out of the tropics, the possibility of sustaining a low-end ECS<sup>34–36</sup> at the same time as a strong shortwave cloud feedback<sup>29–33</sup>, and an enhancement of the hydrological sensitivity<sup>41–44</sup>, while present-day climate remains plausible overall. We suggest that apparent discrepancies between models and observations could be a consequence of the fact that the current climate models systematically miss the effects of convective organization and its dependence on temperature.

### Methods

**Data sources.** Surface temperature data are from HadCRUT 4.3.0.0 from <http://www.cru.uea.ac.uk/>, satellite radiation data from CERES-EBAF 2.8 are from <http://ceres.larc.nasa.gov/>, CMIP5 model outputs are obtained from <http://esgf-data.dkrz.de/>. Relevant model output is available on request from [publications@mpimet.mpg.de](mailto:publications@mpimet.mpg.de).

**Code availability.** The ECHAM6 atmosphere model is distributed on <http://www.mpimet.mpg.de/>. The code changes to introduce an iris effect and to calculate feedback with PRP (revision 2885) are available on request from [publications@mpimet.mpg.de](mailto:publications@mpimet.mpg.de).

Received 23 September 2014; accepted 13 March 2015; published online 20 April 2015

## References

- Lindzen, R. S., Chou, M.-D. & Hou, A. U. Does the Earth have an adaptive infrared iris? *Bull. Am. Meteorol. Soc.* **82**, 417–432 (2001).
- Hartmann, D. L. & Michelsen, M. L. No evidence for iris. *Bull. Am. Meteorol. Soc.* **83**, 249–254 (2002).
- Lau, K. M. & Wu, H. T. Warm rain processes over tropical oceans and climate implications. *Geophys. Res. Lett.* **30**, 1944–8007 (2003).
- Rapp, A. D., Kummerow, C., Berg, W. & Griffith, B. An evaluation of the proposed mechanism of the adaptive infrared iris hypothesis using TRMM VIRS and PR measurements. *J. Clim.* **18**, 4185–4194 (2005).
- Rondanelli, R. & Lindzen, R. S. Observed variations in convective precipitation fraction and stratiform area with sea surface temperature. *J. Geophys. Res.* **113**, D16119 (2008).
- Lindzen, R. S. & Choi, Y.-S. On the determination of climate feedbacks from ERBE data. *Geophys. Res. Lett.* **36**, L16705 (2009).
- Trenberth, K. E., Fasullo, J. T., O'Dell, C. & Wong, T. Relationships between tropical sea surface temperature and top-of-atmosphere radiation. *Geophys. Res. Lett.* **37**, L03702 (2010).
- Lindzen, R. S. & Choi, Y.-S. On the observational determination of climate sensitivity and its implications. *Asia-Pacif. J. Atmos. Sci.* **47**, 377–390 (2011).
- Su, H. *et al.* Variations of tropical upper tropospheric clouds with sea surface temperature and implications for radiative effects. *J. Geophys. Res.* **113**, D10211 (2008).
- Rondanelli, R. & Lindzen, R. S. Comment on 'Variations of tropical upper tropospheric clouds with sea surface temperature and implications for radiative effects by H. Su *et al.*'. *J. Geophys. Res.* **115**, D06202 (2009).
- Collins, M. *et al.* in *Climate Change 2013: The Physical Science Basis*. (eds Stocker, T. F. *et al.*) 1029–1136 (IPCC, Cambridge Univ. Press, 2013).
- Fu, Q., Baker, M. & Hartmann, D. L. Tropical cirrus and water vapor: An effective Earth infrared iris feedback? *Atmos. Chem. Phys.* **2**, 31–37 (2002).
- Lin, B., Wielicki, B. A., Chambers, L. H., Hu, Y. & Xu, K.-M. The iris hypothesis: A negative or positive cloud feedback? *J. Clim.* **15**, 3–7 (2002).
- Dessler, A. E. Observations of climate feedbacks over 2000–10 and comparison to climate models. *J. Clim.* **26**, 333–342 (2013).
- Forster, P. M. & Gregory, J. M. The climate sensitivity and its components diagnosed from earth radiation budget data. *J. Clim.* **19**, 39–52 (2006).
- Block, K. & Mauritsen, T. Forcing and feedback in the MPI-ESMLR coupled model under abruptly quadrupled CO<sub>2</sub>. *J. Adv. Model. Earth Syst.* **5**, 1–16 (2013).
- Clement, A. C. & Soden, B. The sensitivity of the tropical-mean radiation budget. *J. Clim.* **18**, 3189–3203 (2005).
- Nilsson, J. & Emanuel, K. Equilibrium atmospheres of a two-column radiative-convective model. *Q. J. R. Meteorol. Soc.* **125**, 2239–2264 (1999).
- Emanuel, K., Wing, A. A. & Vincent, E. M. Radiative-convective instability. *J. Adv. Model. Earth Syst.* <http://dx.doi.org/10.1002/2013MS000270> (2014).
- Trenberth, K. E. Atmospheric moisture residence times and cycling: Implications for rainfall rates and climate change. *Clim. Change* **39**, 667–694 (1998).
- Bretherton, C. S., Blossey, P. N. & Khairoutdinov, M. An energy balance analysis of deep convective self-aggregation above uniform SST. *J. Atmos. Sci.* **62**, 4273–4292 (2005).
- Tobin, I., Bony, S. & Roca, R. Observational evidence for relationship between the degree of aggregation of deep convection, water vapor, surface fluxes and radiation. *J. Clim.* **25**, 6885–6904 (2012).
- Muller, C. J. & Held, I. M. Detailed investigation of the self-aggregation of convection in cloud-resolving simulations. *J. Clim.* **69**, 2551–2565 (2012).
- Satoh, M., Iga, S.-I., Tomita, H., Tsushima, Y. & Noda, A. T. Response of upper clouds in global warming experiments obtained using a global nonhydrostatic model with explicit cloud processes. *J. Clim.* **25**, 2178–2191 (2012).
- Tsushima, Y. *et al.* High cloud increase in a perturbed SST experiment with a global nonhydrostatic model including explicit convective processes. *J. Adv. Model. Earth Syst.* <http://dx.doi.org/10.1002/2013MS000301> (2014).
- Klocke, D., Pincus, R. & Quaas, J. On constraining estimates of climate sensitivity with present-day observations through model weighting. *J. Clim.* **24**, 6092–6099 (2011).
- Stevens, B. & Bony, S. Water in the atmosphere. *Phys. Today* **66** (6), 29–34 (2013).
- Vial, J., Dufresne, J.-L. & Bony, S. On the interpretation of inter-model spread in CMIP5 climate sensitivity estimates. *Clim. Dyn.* **41**, 3339–3362 (2013).
- Clement, A., Burgman, R. & Norris, J. Observational and model evidence for positive low-level cloud feedback. *Science* **325**, 460–464 (2009).
- Rieck, M., Nuijens, L. & Stevens, B. Marine boundary layer cloud feedbacks in a constant relative humidity atmosphere. *J. Atmos. Sci.* **69**, 2538–2550 (2012).
- Fasullo, J. T. & Trenberth, K. E. A less cloudy future: The role of subtropical subsidence in climate sensitivity. *Science* **338**, 792–794 (2012).
- Sherwood, S. C., Bony, S. & Dufresne, J.-L. Spread in model climate sensitivity traced to atmospheric convective mixing. *Nature* **505**, 37–42 (2014).
- Su, H. *et al.* Weakening and strengthening structures in the Hadley Circulation change under global warming and implications for cloud response and climate sensitivity. *J. Geophys. Res. Atmos.* **119**, 5787–5805 (2014).
- Otto, A. *et al.* Energy budget constraints on climate response. *Nature Geosci.* **6**, 415–416 (2013).
- Skeie, R. B., Berntsen, T., Aldrin, M., Holden, M. & Myhre, G. A lower and more constrained estimate of climate sensitivity using updated observations and detailed radiative forcing time series. *Earth Syst. Dynam.* **5**, 139–175 (2014).
- Lewis, N. & Curry, J. A. The implications for climate sensitivity of AR5 forcing and heat uptake estimates. *Clim. Dynam.* <http://doi.org/3hn> (2014).
- Haimberger, L., Tavolato, C. & Sperka, S. Homogenization of the global radiosonde temperature dataset through combined comparison with reanalysis background series and neighboring stations. *J. Clim.* **25**, 8108–8131 (2012).
- Po-Chedley, S. & Fu, Q. Discrepancies in tropical upper tropospheric warming between atmospheric circulation models and satellites. *Environ. Res. Lett.* **7**, 044018 (2012).
- Newell, R. E., Herman, G. F., Gould-Stewart, S. & Tanaka, M. Decreased global rainfall during the past ice age. *Nature* **253**, 33–34 (1975).
- Held, I. M. & Soden, B. J. Robust responses of the hydrological cycle to global warming. *J. Clim.* **19**, 5686–5699 (2006).
- Zhang, X. *et al.* Detection of human influence on twentieth-century precipitation trends. *Nature* **448**, 461–466 (2007).
- Lambert, F. H., Stine, A. R., Krakauer, N. Y. & Chiang, J. C. H. How much will precipitation increase with global warming? *EOS* **89**, 193200 (2008).
- Durack, P. J., Wijffels, S. E. & Matear, R. J. Ocean salinities reveal strong global water cycle intensification during 1950 to 2000. *Science* **336**, 455–458 (2012).
- Ren, L., Arkin, P., Smith, T. M. & Shen, S. S. P. Global precipitation trends in 1900–2005 from a reconstruction and coupled model simulations. *J. Geophys. Res. Atmos.* **118**, 1679–1689 (2013).
- Johanson, C. M. & Fu, Q. Hadley cell widening: Model simulations versus observations. *J. Clim.* **22**, 2713–2725 (2009).
- Shindell, D. T. Inhomogeneous forcing and transient climate sensitivity. *Nature Clim. Change* **4**, 274–277 (2014).
- Santer, B. D. *et al.* Volcanic contribution to decadal changes in tropospheric temperature. *Nature Geosci.* **7**, 185–189 (2014).
- Trenberth, K. E. & Fasullo, J. T. Tracking Earth's energy. *Science* **328**, 316–317 (2010).
- Ramanathan, V., Crutzen, P. J., Kiehl, J. T. & Rosenfeld, D. Aerosols, climate, and the hydrological cycle. *Science* **294**, 2119–2124 (2001).
- Llovel, W., Willis, J. K., Landerer, F. W. & Fukumori, I. Deep-ocean contribution to sea level and energy budget not detectable over past decade. *Nature Clim. Change* **4**, 1031–1035 (2014).

## Acknowledgements

Contributions from S. Bony, P. Forster, Quiang Fu, A. Gettelman, J. Gregory, I. Held, S. Klein, R. Lindzen, R. Pierrehumbert, S. Po-Chedley, D. Popke, F. Rauser, S. Sherwood and M. Zelinka were valuable in advancing this study. CERES data were obtained from the NASA Langley Research Center, HadCRUT4 data are provided by the Met Office Hadley Centre and the Climatic Research Unit at the University of East Anglia, and CMIP5 data from the coupled modelling groups (Supplementary Table 3) coordinated by the World Climate Research Programme's Working Group on Coupled Modelling. This work was supported by the Max-Planck-Gesellschaft (MPG) and by funding through the EUCLIPSE project from the European Union, Seventh Framework Programme (FP7/2007–2013) under grant agreement no. 244067. Computational resources were made available by Deutsches Klimarechenzentrum (DKRZ) through support from Bundesministerium für Bildung und Forschung (BMBF).

## Additional information

Supplementary information is available in the [online version of the paper](#). Reprints and permissions information is available online at [www.nature.com/reprints](http://www.nature.com/reprints). Correspondence should be addressed to T.M.